

Supporting Information

Dynamics of excited-state conformational relaxation and electronic delocalization in conjugated porphyrin oligomers

Ming-Hua Chang, Markus Hoffmann, Harry L. Anderson, and Laura M. Herz

Table of Contents

Figure S1. $^1\text{H-NMR}$ diffusion constants of \mathbf{P}_n and \mathbf{C}_8	S1
Figure S2. GPC traces of \mathbf{P}_n	S2
Figure S3. MALDI-ToF spectrum of \mathbf{C}_8	S2
Figure S4. $^1\text{H-NMR}$ spectrum of \mathbf{C}_8	S3
Figure S5. UV-Vis titration data for the formation of \mathbf{C}_8	S4
Figure S6. UV-Vis titration data for the formation and break-up of \mathbf{L}_8	S4
Figure S7. Binding isotherm and calculated curve for the break-up of \mathbf{L}_8	S5
Equations S1-S7. Fitting equations for the break-up of \mathbf{L}_8 with excess BiPy	S5
Figure S8. Molecular mechanics geometry optimization of \mathbf{C}_8	S6
Figure S9. Molecular mechanics geometry optimization of \mathbf{L}_8	S6
Figure S10. $^1\text{H-NMR}$ spectrum of \mathbf{P}_8	S7
Figure S11. MALDI-ToF spectrum of \mathbf{P}_8	S7

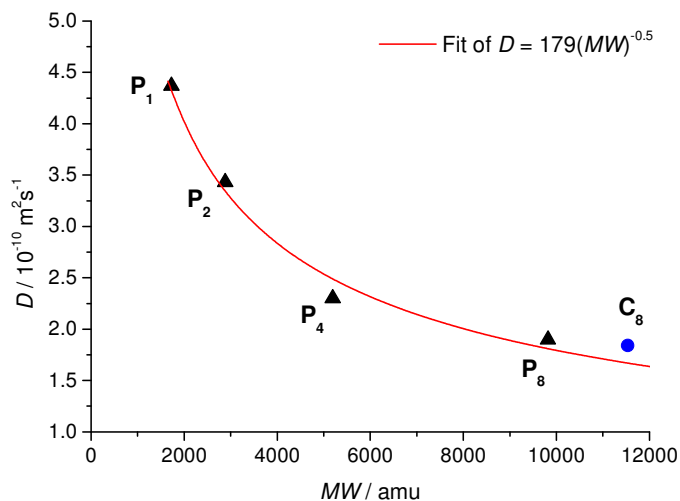


Figure S1. $^1\text{H-NMR}$ diffusion constant, D vs. formula molecular weight for single-stranded porphyrin oligomers, \mathbf{P}_n (\blacktriangle) and cyclic octamer, \mathbf{C}_8 (\bullet) (CDCl_3 + 1% D_5 -pyridine, 298 K, 500 MHz). The smooth curve shows a fit to $D \propto MW^{-0.5}$ which is expected for a spherical molecule. This is probably because the oligomers are relatively rigid, but have long flexible side-chains. The diffusion coefficient for \mathbf{C}_8 confirms that it is a 1:1 complex. The fit for $\mathbf{P}_1 - \mathbf{P}_8$ indicates the absence of aggregates.

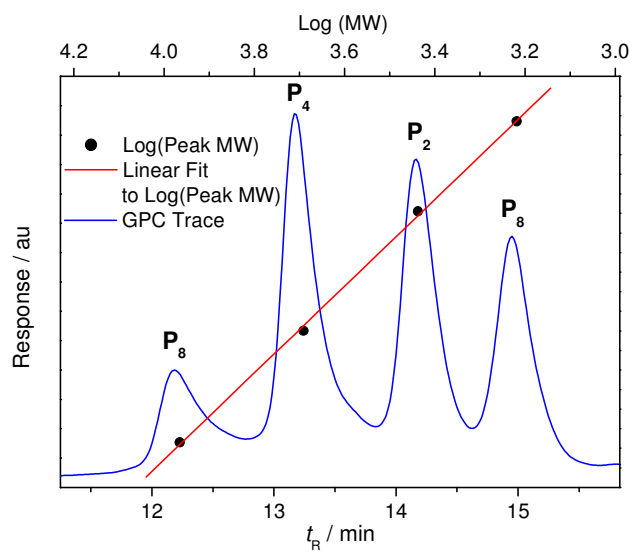


Figure S2. Analytical GPC traces of single-stranded porphyrin oligomers in THF (absorption signal at 255 nm; flow rate 1 mL min⁻¹; 298 K; 2 x 300 mm, 7.5 mm ID PLgel Mixed-E columns, Polymer Laboratories Ltd.). The good fit to $t_R \propto \log(MW)$ confirms the absence of aggregates.

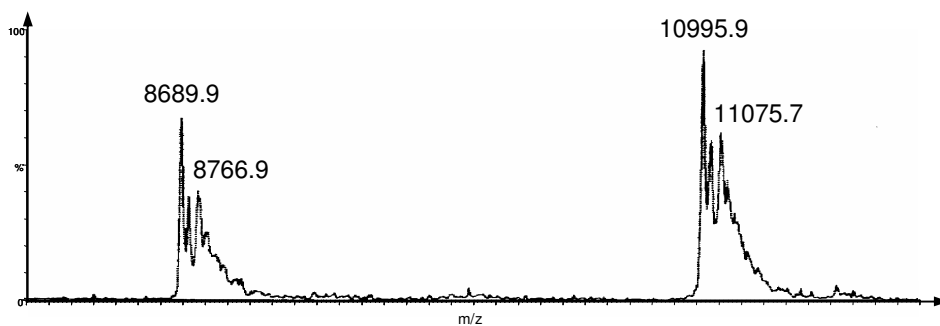


Figure S3. MALDI-ToF mass spectra of **C₈** (expected mass **C₈** 10985.2, found 10995.9; expected mass deprotected **P₈** 8680.4, found 8689.9), recorded in positive linear mode with *trans*-2-[3-(4-*tert*-butylphenyl)-2-methyl-2-propenylidene]- malononitrile (DCTB) as matrix.

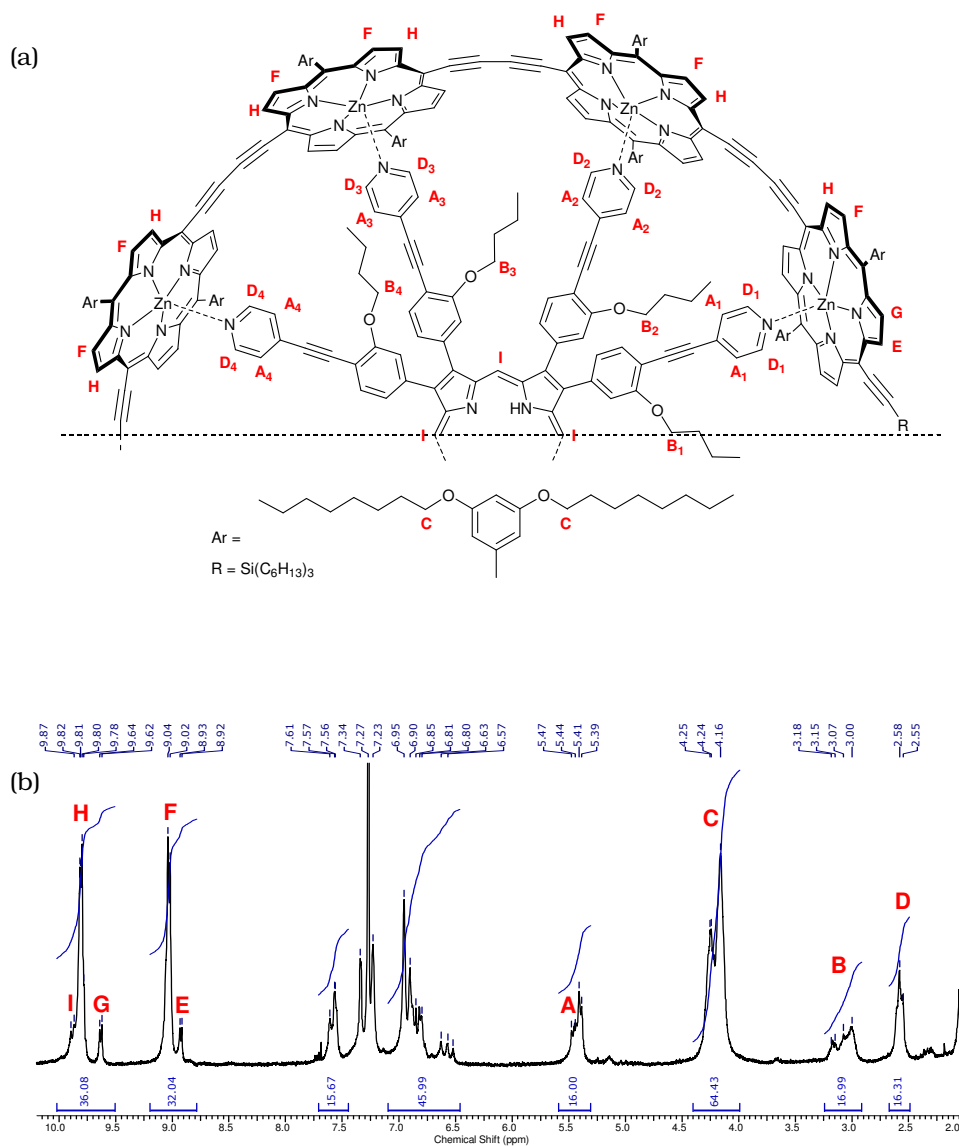


Figure S4. (a) Structure of template · trihexylsilyl-protected octamer complex **C₈**. The dashed line represents a plane of symmetry. (b) ¹H-NMR spectrum of **C₈** (500 MHz, 298 K, CDCl₃, assigned by 2D-COSY and NOESY experiments). The low symmetry of the environment results in splitting of the template resonances, as expected. The integrations shown on these spectra confirm the 1:1 stoichiometry of the complex. The spectrum also confirms that all eight pyridyl sites are coordinated to zinc, e.g. through observation of the α-pyridyl resonances (D₁, D₂, D₃ and D₄) at 2.5 ppm.

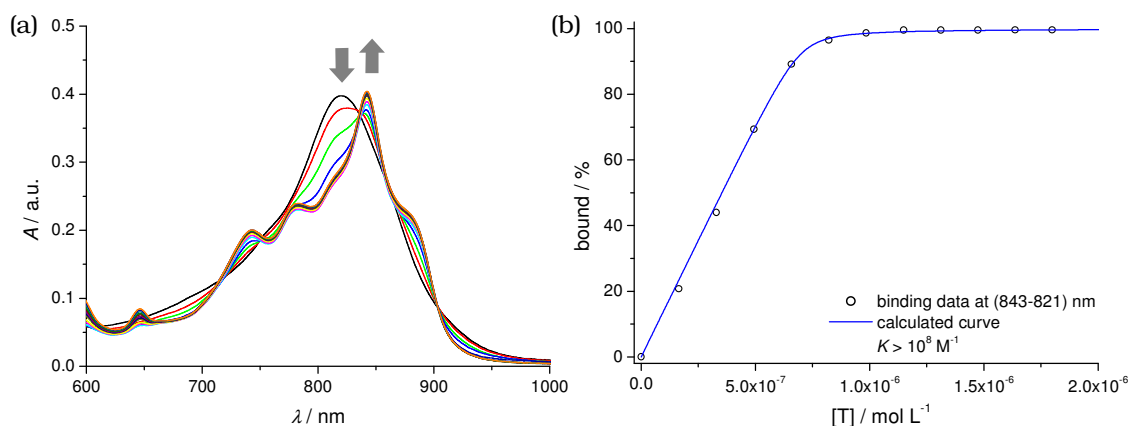


Figure S5. (a) UV-vis titration for the formation of \mathbf{C}_8 from template and pyridine-free linear porphyrin octamer, \mathbf{P}_8 ($[\mathbf{P}_8] = 1.8 \mu\text{M}$, 298 K, CHCl_3). (b) Binding isotherm obtained from the absorbance data at (843-821) nm. The data were fitted to a 1:1 binding isotherm to give a binding constant of $K > 10^8 \text{ M}^{-1}$. Arrows indicate areas of increasing and decreasing absorption during the titration. The isosbestic UV-vis spectra and sharp end-point indicate that it is essentially a two-state equilibrium, without significant concentrations of intermediates.

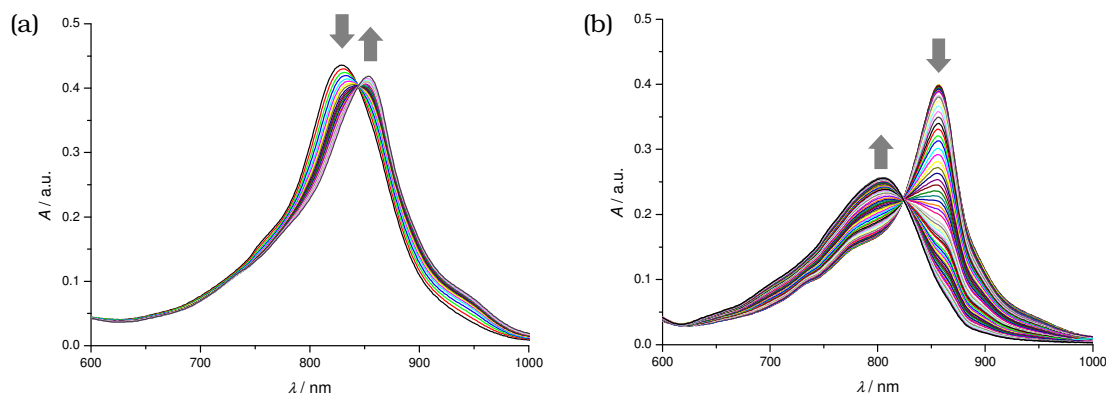


Figure S6. UV-vis titration for (a) the formation of \mathbf{L}_8 from BiPy and pyridine-free linear porphyrin octamer, \mathbf{P}_8 ($[\mathbf{P}_8] = 0.54 \mu\text{M}$, 298 K, CHCl_3) and (b) the break-up of the octamer ladder complex with excess BiPy ($[\mathbf{P}_8] = 0.49 \mu\text{M}$, 303 K, CHCl_3). Arrows indicate areas of increasing and decreasing absorption during the titration. The titration curves show simple isosbestic behaviour and sharp end-points. This indicates that both processes are essentially two-state equilibria, without significant concentrations of intermediates. The close similarities of the spectra of \mathbf{L}_8 with those of previously studied 4,4'-BiPy ladders^[1] derived from closely related porphyrin oligomers supports the structured assignment of those assemblies.

[1] *J. Am. Chem. Soc.* **2006**, *128*, 12432; *J. Am. Chem. Soc.* **2007**, *129*, 13370; *J. Mater. Chem.* **2003**, *13*, 2796; *J. Am. Chem. Soc.* **2002**, *124*, 9712; *J. Am. Chem. Soc.* **1999**, *121*, 11538; *Inorg. Chem.* **1994**, *33*, 972.

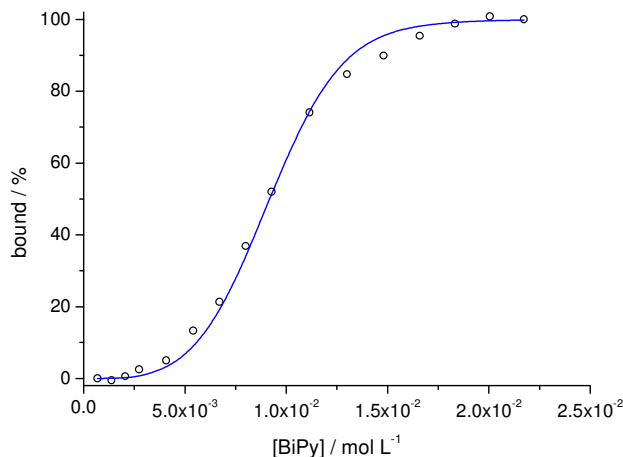


Figure S7. Binding isotherm obtained from the break-up titration of **L₈** with excess BiPy (**[P₈]** = 0.49 μ M, 303 K, CHCl₃). The cuvette was heated to 50 °C for 10 minutes between each aliquot addition to achieve equilibrium. The titration data for the ladder-breaking equilibrium at 825 nm were analyzed using eqs (S1)–(S7), where **O** is porphyrin octamer **P₈** and BiPy is 4,4'-bipyridine. This fitting equation approximates the total concentration of BiPy (**[BiPy]** = **[BiPy]₀**). This is valid since the concentration of bound BiPy is >1000 times less than the concentration of free BiPy. The binding isotherm fits well to the calculated curve for a two-state equilibrium. Fitting gives a binding constant of $K = 9.3 \times 10^9 \text{ M}^{-7}$.



$$K = \frac{[\text{OBiPy}_8]^2}{[\text{O}_2\text{BiPy}_8][\text{BiPy}]^8} \quad (\text{S2})$$

$$[\text{O}]_0 = 2[\text{O}_2\text{BiPy}_8] + [\text{OBiPy}_8] \quad (\text{S3})$$

$$K[\text{O}_2\text{BiPy}_8][\text{BiPy}]_0^8 - ([\text{O}]_0 - 2[\text{O}_2\text{BiPy}_8])^2 = 0 \quad (\text{S4})$$

$$[\text{O}_2\text{BiPy}_8] = \frac{[\text{O}]_0}{2} + \frac{K[\text{BiPy}]_0^8}{8} + \frac{\sqrt{K^2[\text{BiPy}]_0^{16} + 8K[\text{BiPy}]_0^8[\text{O}]_0}}{8} \quad (\text{S5})$$

$$[\text{OBiPy}_8] = [\text{O}]_0 - 2[\text{O}_2\text{BiPy}_8] \quad (\text{S6})$$

$$y = \frac{[\text{OBiPy}_8]}{[\text{O}]_0} = \frac{K[\text{BiPy}]_0^8 + \sqrt{K^2[\text{BiPy}]_0^{16} + 8K[\text{BiPy}]_0^8[\text{O}]_0}}{4[\text{O}]_0} \quad (\text{S7})$$

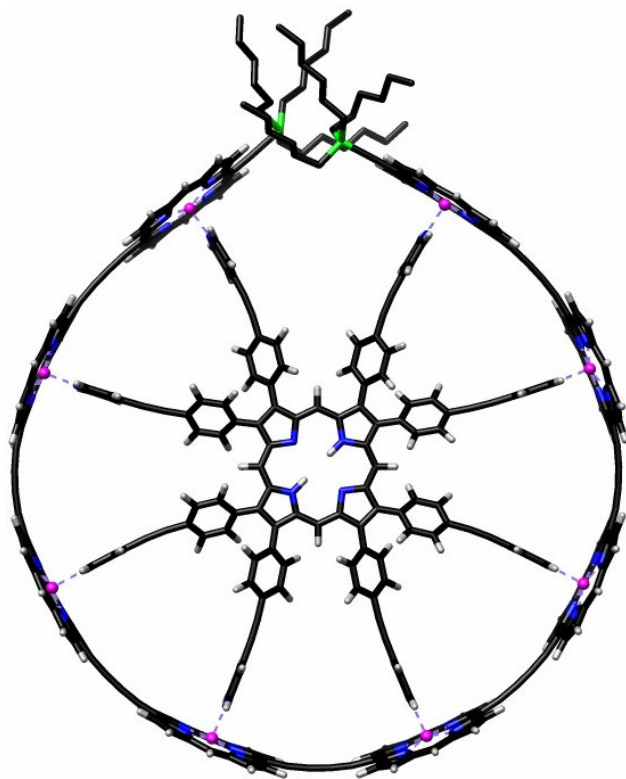


Figure S8. Geometry of **C₈** obtained by molecular mechanics geometry optimization (*meso*-aryl substituents omitted for clarity; calculated using the MM+ force-field, HyperChem 8.0, HyperCube, Inc., USA).

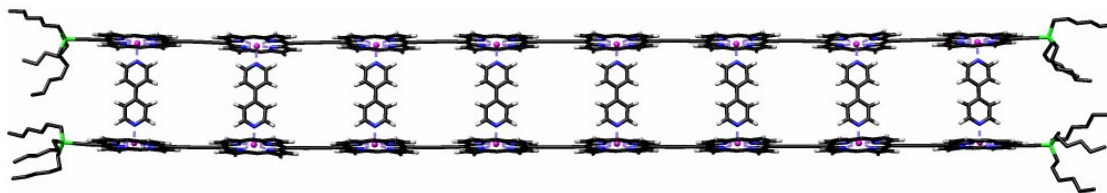


Figure S9. Geometry of **L₈** obtained by molecular mechanics geometry optimization (*meso*-aryl substituents omitted for clarity; calculated using the MM+ force-field, HyperChem 8.0, HyperCube, Inc., USA).

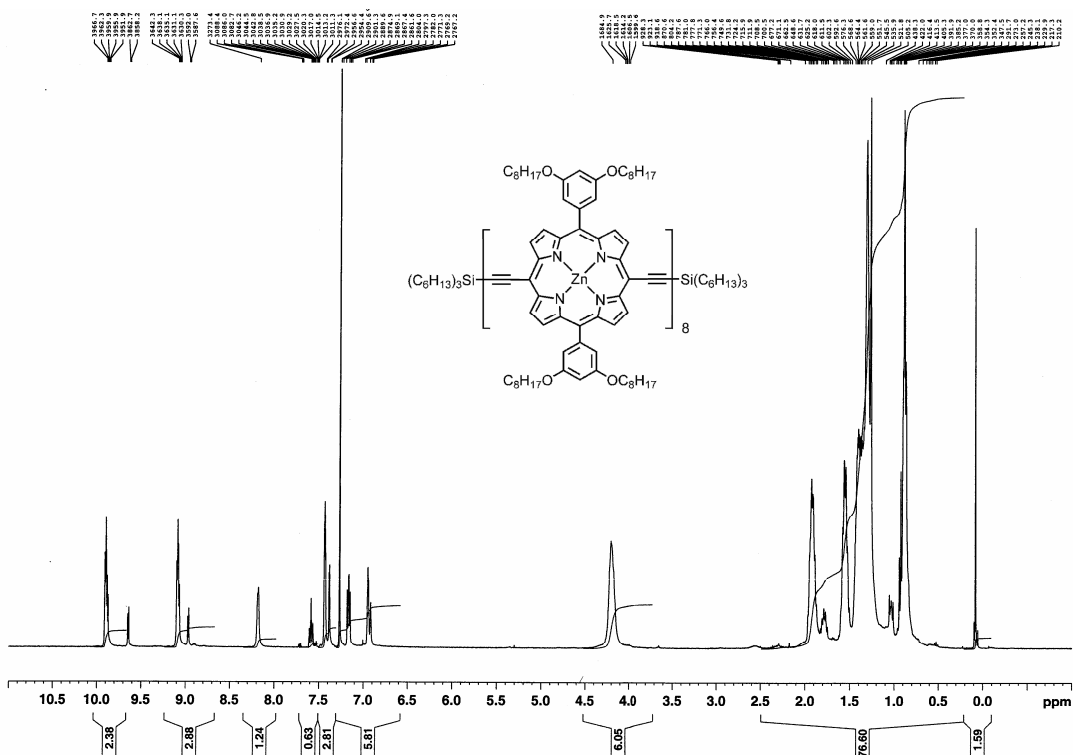


Figure S10. 1H -NMR spectrum of **P₈** (400 MHz, 298 K, $CDCl_3$ / 1% D_5 -pyridine).

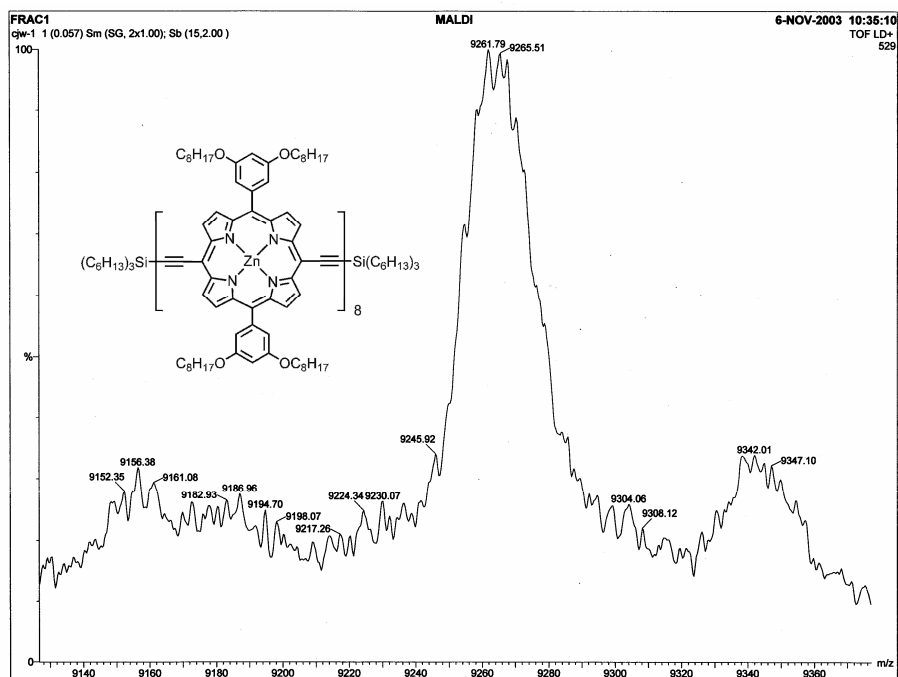


Figure S11. MALDI-ToF mass spectra of **P₈** (expected mass **P₈** 9245.5, found 9261.8), recorded in positive linear mode with *trans*-2-[3-(4-*tert*-butylphenyl)-2-methyl-2-propenylidene]-malononitrile (DCTB) as matrix.